

Likely, Light, and Accurate Context-Free Clusters-based Trajectory Prediction

Tiago Rodrigues de Almeida and Oscar Martinez Mozos

Abstract— Autonomous systems in the road transportation network require intelligent mechanisms that cope with uncertainty to foresee the future. In this paper, we propose a multi-stage probabilistic approach for trajectory forecasting: trajectory transformation to displacement space, clustering of displacement time series, trajectory proposals, and ranking proposals. We introduce a new deep feature clustering method, underlying self-conditioned GAN, which copes better with distribution shifts than traditional methods. Additionally, we propose novel distance-based ranking proposals to assign probabilities to the generated trajectories that are more efficient yet accurate than an auxiliary neural network. The overall system surpasses context-free deep generative models in human and road agents trajectory data while performing similarly to point estimators when comparing the most probable trajectory.

I. INTRODUCTION

For a wide range of applications, an accurate estimation of the future position of moving agents is paramount. In the transportation sector, several branches benefit from effective forecasting systems such as (1) flexible, reliable and robust road traffic network relies on the prediction of traffic to prevent congestion and provide safety and efficiency [1], [2]; (2) Advanced Driver Assistance Systems (ADAS) capable of foreseeing the future can then adapt accordingly [3]; (3) the task of transporting goods may resort to a simulation of the future, which foster more informed planning and resource allocation [4]. Further, trajectory prediction enhances situational awareness in complex dynamic environments such as industrial facilities, public sites, or home environments where multiple agents are moving. Finally, multimodal probabilistic forecasting of trajectories yields a richer representation of possible future events, which triggers subsequent decision-making systems [5].

The trajectory forecasting task mainly underlies three pillars such as agents interactions modeling [6]–[11], semantic context learning [12], [13], and multimodal predictions [14]–[16]. Also, multimodal approaches brought a new view to the trajectory prediction domain as accounting for a set of diverse behaviors, instead of a unique point estimate, offers a much more reasonable and safe solution [17]. The problem with previous approaches is that they do not provide probabilistic or score measures for each trajectory estimate. In these cases, depending on the model’s variability (induced

This work was supported by the Wallenberg AI, Autonomous Systems and Software Program (WASP) funded by the Knut and Alice Wallenberg Foundation.

The authors are with Center for Applied Autonomous Sensor Systems (AASS), Örebro University, Örebro, Sweden {tiago.almeida, oscar.mozos}@oru.se

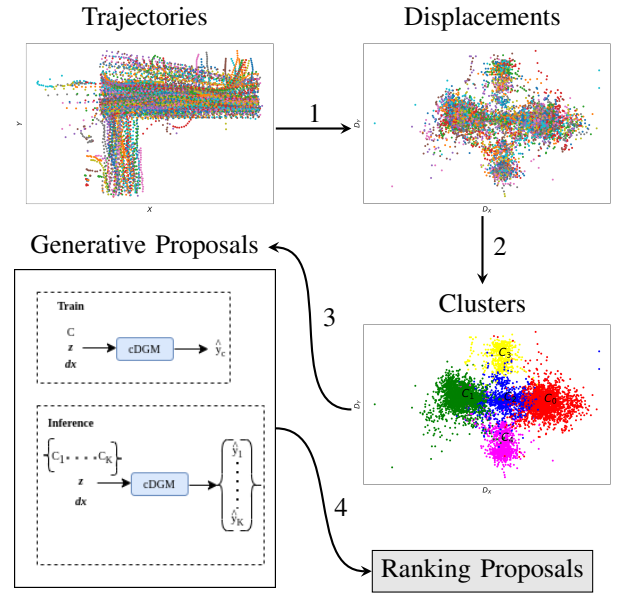


Fig. 1. System overview. (1) We transform spatiotemporal trajectory data into the displacement space. (2) We cluster the displacement data into K partitions. (3) We train deep generative models that take as inputs the displacements (dx), the respective cluster class (C), and white noise (z). During inference, those models propose K predictions, being K the number of clusters. (4) We proceed to the ranking proposals step, where we assign probabilities to the predicted trajectories.

usually by the *k*-variety loss [17]), the predictions can be considered accurate or not [11]. Most works following previous benchmarks [18] opt by sampling K trajectories (usually, $K = 20$) and evaluating the closest to the ground truth. The premise that the closest trajectory to the ground truth can give a reasonable overview of the forecaster’s performance is ambiguous as the model’s variability plays a major role in the reported results [11]. Therefore, the research community urges probabilistic and accurate predictions with adequate results reporting. In addition, context-agnostic approaches have had little attention from the research community [19]–[21], which we see as a gap to explore novel strategies for adding trajectory-based information to improve current context-free methods.

Following recent works [22]–[24], our method encompasses multiple stages where the final objective is to provide a distribution of trajectories and the respective probabilities. To that end, our system sequentially clusters the input data, trains a conditional Deep Generative Model (cDGM) to map the input data and clusters’ ids to the respective future trajectory, and assigns likelihoods to the trajectories in a post-hoc

fashion (see Fig. 1). The clusters ids aim to represent akin similar behaviors that drive the final predictions whereas the ranking proposals methods allow us to assign probabilities to each generated trajectory. In this way, we can provide diverse and probabilistic accurate predictions. Furthermore, inspired by [11], we consider Top-3 scores for the assessment and comparison of methods. Previous works have considered the Top-20 trajectories, which we agree can mislead the interpretation of the results.

In summary, this work aims to improve standalone context-free Deep Generative Models by adding trajectory-related information encoded in the conditioning cluster class. Inspired by [25], [26], our first contribution is a novel deep generative clustering algorithm, Full Path Self-Conditioned GAN (FP SC-GAN). Besides clustering the input data, this framework generates complete sets of displacements that can be part of a downstream data augmentation process. However, in this work, we solely focus on the clustering capability of FP SC-GAN. Alternatively to [22]–[24], our second contribution is the distance-based ranking proposals methods, which do not rely on training an auxiliary neural network but are still rather effective and efficient. The proposed distance-based ranking proposals methods uniquely require access to the clustering space. In this work, these methods perform likewise to an auxiliary deep neural network, and run in *linear time* whereas a Multilayer Perceptron (MLP) requires *quadratic time*. Finally, to the best of our knowledge, we propose the first quantitative metrics report where the likelihoods provided by the system directly affect the Top-3 trajectory prediction metrics.

II. RELATED WORK

Trajectory forecasting has been predominantly researched on two fronts: context-agnostic and context-aware approaches. Context-agnostic methods solely forecast based on observed trajectory patterns, whereas context-aware methods include social and scene layout cues. While context-agnostic approaches have received little attention [19]–[21] from the research community, context-aware methods have been comprehensively investigated [6], [11], [17], [27]–[29]. This paper focuses on context-agnostic approaches and breeding mechanisms for probabilistic trajectory forecasting based on encoded clustering information.

In the trajectory generation domain, some works tackled the problem from a probabilistic view in road scenarios [30]–[33] and human trajectory data [22]–[24]. CoverNet [30] comprises a Convolutional Neural Network (CNN) to extract contextual features from a road scene and a trajectory generator module to produce a set of possible predictions. Then, the system directly classifies the set of plausible trajectories yielding the score of each prediction. Conversely, we aim to produce context-agnostic samples to open the domain of applications of our system and reduce its requirements. In [31], the authors propose a post-hoc method named Likelihood-Based Diverse Sampling (LDS). In that paper, a novel objective function and a non-i.i.d sampling method

encourage diverse predictions by suppressing similar predictions from the generated set of samples and leveraging the likelihoods from a pre-trained generative model. However, this work does not determine the scores (likelihoods) of the set of plausible trajectories, which we claim is paramount for risk-aware downstream decision processes. *HAICU* [32] is a system that relies on perception and classification modules to give the class distribution of road agents. This system stands for a Conditional Variational Autoencoder (cVAE) conditioned on the class distribution and the observed trajectory of road agents to produce multimodal predictions. Therefore, this work heavily relies on upstream supervised methods to yield the class distribution, which is not easily generalizable to human trajectory data. To cope with this limitation, we propose unsupervised techniques to cluster akin trajectories, which we consider agnostic to the trajectory domain and more generalizable. In [33], the authors enforce underlying physical admissibility constraints and diversity in a post-hoc trajectory sampling process based on a determinantal point process (DDP). Although it proposes a robust strategy for considering context using admissibility constraints induced in the objective function, it does not provide a probabilistic view of the predicted trajectories. [22] devises a three-step method based on clustering, classification, and synthesis to predict. Contrarily to this work, we first predict by using a cDGM and then propose a ranking proposals step. In this work, we investigate ranking proposals methods based on the distance to the already conceived clustering space and, therefore, not relying on a classification network. Further, [23] proposes a method based on clustered goal points and a final classification step. While both [22] and [23], at the classification step, learn the mapping between the past trajectory and the cluster class, we rank complete trajectories emphasizing the generated *tracklets*. Finally, in [24], the authors investigated a system with two branches: a motion pattern selector and a multimodal trajectory generator. The former produces a *gallery* of diverse motion patterns, while the latter refines them and generates future trajectories. Then, a scoring method produces the most diverse predictions.

Our work encompasses mechanisms under the same umbrella as [22]–[24], but our main objective is to propose a system that can improve current deep generative models by including information from clustered data. In our system the clusters drive the multimodality, and the ranking proposals methods run on the generated trajectories. In addition, our distance-based ranking proposals methods does not rely on training any auxiliary neural network conversely to previous works [22]–[24]. In our case, the ranking proposals step depends exclusively on the intrinsic nature of the clustering space and a similarity measure to the generated trajectories. Further, we propose a new deep clustering method inspired by a self-supervised deep generative model developed for the image generation task [25]. Finally, contrarily to previous works, the probabilities of each trajectory strongly affect the evaluation of our method, while in previous works, the probabilities only give a sense of the likelihood of each particular event.

III. METHODOLOGY

The objective of our system (see Fig. 1) is to offer accurate and probabilistic future estimations for trajectory data. Succinctly, it comprises four sequential steps: (1) transformation to the displacement space, (2) clustering step, (3) deep generative proposals, and (4) ranking proposals step. To gain a comprehensive understanding of each component, this section provides a detailed description of the problem we address and an overview of our proposed solution. Subsequently, we delve into the displacement transformation and clustering steps. In the succeeding subsection, we outline the process of acquiring the proposals. Lastly, we introduce the ranking proposals step, which assigns probabilities to the set of predicted outputs.

A. Problem Statement and System Overview

Most trajectory forecasting models generate a set of plausible futures, $\{\hat{y}_i\}^K$, given an observed *tracklet*, \mathbf{x} . The observed *tracklet* is an evenly spaced time series of T_O observations in the XY -plane. Ultimately, the forecasting models' goal is to predict the future behavior of the input time series for a certain horizon of T_P time steps. In this paper, we go beyond the trajectory generative process and also propose a post-hoc method to assign probabilities, $\{\hat{p}_i\}^K$, to the respective K proposed trajectories. In this way, besides future plausible trajectories we also provide the likelihood of each trajectory. We consider the system's starting point a dataset composed of N_T trajectories.

In the first step of our system, we transform the input trajectories into the displacement space. As a result, we also perform any prediction in the displacement space. In doing so, we avoid dependence on the spatial context where the input data lies. Therefore, any downstream task is more generalizable to new domains. Then, we cluster the displacement input vectors into K partitions via clustering. This step is paramount in the system as it groups akin time series of displacements that we feed into the generation process of future displacements. Consequently, we propose to train cDGMs, such as a cVAE or a Conditional Generative Adversarial Network (cGAN) to learn the future displacements given the observed displacements and the respective cluster class, c (i.e., the identifier for the cluster class conceived with the ground truth displacements). As we cluster the entire set of displacements, after training the cDGM, there will be a link between the prediction and both the observed displacement *tracklet* and the respective cluster class. Assuming a successful clustering and cDGM's training steps, this link allows us to claim that the prediction generated from the cluster class c will be more similar to the group of trajectories in c than the trajectories from any other cluster. Thus, during inference, we propose to generate K future displacement vectors (one per cluster class) and use a ranking method to assign likelihoods to the proposed future displacements. The idea behind the ranking method is to assign high likelihoods to displacement vectors that resemble the ones on the respective ground truth cluster and do the opposite for the remaining ones. For instance,

assuming that the right cluster class is c_i , our key insight is that the produced sample for c_i , \hat{dy}_i , will be more similar to the ground truth displacements on c_i than any prediction in $\{\hat{dy}_j\}_{j=1 \setminus i}^K$ to the respective ground truth displacements in each of the clusters in $\{c_j\}_{j=1 \setminus i}^K$.

B. Displacement Transformation and Clustering Step

Primarily, our method transforms the raw trajectory data, $\mathbf{x} \oplus \mathbf{y}$, into displacement vectors, $\mathbf{D} \in \mathbb{R}^{N_T \times (T_O + T_P) \times 2}$, where each displacement vector is given by $\mathbf{d} = \mathbf{dx} \oplus \mathbf{dy}$ or formally the finite differences of the observed positions:

$$s = \{(d_x, d_y)^1, \dots, (d_x, d_y)^{T_P}\}, \quad (1)$$

being the superscript the time step.

At the clustering step, we group \mathbf{D} into sub-partitions of akin displacements, $\{\mathbf{d}_j\}_{j=1}^K$, where \mathbf{d}_j is a set itself with arbitrary cardinality (less or equal than N_T). At the end of the clustering step, we guarantee that $\sum_{j=1}^K |\{\mathbf{d}_j\}| = N_T$, i.e., each sample belongs to only one cluster. We evaluate three different clustering methods: *k-Means* [34], *TS k-Means* [35], and our proposed FP SC-GAN. To this end, we feed *k-Means* with flattened displacements vectors in the form of:

$$s_f = \{d_x^1, d_y^1, \dots, d_x^{T_P}, d_y^{T_P}\} \quad (2)$$

We also evaluate the extended version for time series provided by [35], *TS k-Means*. The major differences between these two clustering methods are that for the *TS k-Means*, the input is given by Eq. 1 and the similarity measure is evaluated time-wise (we use *soft-DTW* [36]). Finally, Fig. 2 depicts our proposed deep feature-based clustering method, FP SC-GAN. This architecture is considered a two-fold provider: on one side, it produces the clustering space used in the later forecasting task; on the other side, it generates a complete set of synthetic displacements. This synthetic data can even serve as a data augmentation process, which we do not cover in this work. FP SC-GAN underlies the idea that the discriminator's feature space can be meaningful for downstream tasks [25] (in this case, the clustering task). To that end, FP SC-GAN comprises a conditional generator (G) and a discriminator (D). We condition the generator on a cluster class (c) drawn from the clustering space and white noise (z). Then one MLP-based decoder generates an entire displacement vector, $\hat{\mathbf{d}} = \hat{\mathbf{dx}} \oplus \hat{\mathbf{dy}}$, that should resemble one of the ground truth samples belonging to the conditioning cluster. The discriminator (D) learns to distinguish generated and ground truth samples according to a score (s). During training, to assess the clustering process, we assume that the clustering is as good as the quality of the generated displacements. We consider this a fair proxy as the only deterministic input signal given to the generator is the cluster id. Analogously to [26], we train the FP SC-GAN with the binary cross entropy loss to optimize the discriminator and a weighted sum of the discriminator's loss and the mean squared error (MSE) loss to optimize the generator, given by:

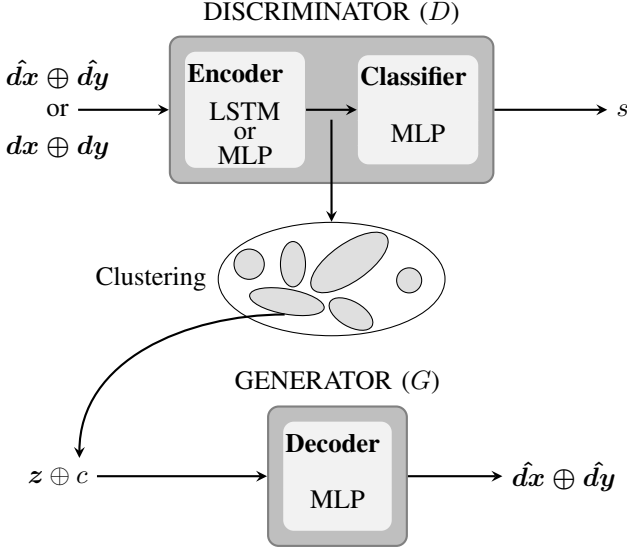


Fig. 2. FP SC-GAN architecture. We pass random noise concatenated with the cluster class, drawn according to the clustering space distribution, to the generator. The generator aims to produce a complete set of displacements. Both generated and real samples pass through the discriminator, which learns to classify them into real or fake. During training, we periodically recluster the discriminator's feature space.

$$L_G = \lambda \text{MSE}(\mathbf{y}, \hat{\mathbf{y}}) + (1 - \lambda) \left(\frac{1}{2} \mathbb{E}[(D(\mathbf{d}) - 1)^2] + \frac{1}{2} \mathbb{E}[D(\hat{\mathbf{d}})^2] \right), \quad (3)$$

being $\hat{\mathbf{y}}$ the entire generated $2D$ trajectory and \mathbf{y} the respective ground-truth, $\hat{\mathbf{d}}$ the generated displacements vector and \mathbf{d} the respective ground truth, and λ the weight applied to the MSE term. For more details on the FP SC-GAN training, we refer the reader to [25], [26].

C. Deep Generative Proposals

To produce potential displacement vectors, we train a cDGM that learns the mapping $\{\mathbf{d}\mathbf{x}, c\} \rightarrow \mathbf{d}\mathbf{y}$. In order to strengthen the validation of our results, we evaluate two cDGMS: a cVAE and a cGAN. In these methods, we first concatenate the cluster class to the input displacement vector. Then, we extract features (f_e) from this joint representation. The next step — noise sampling — is different in cVAE and cGAN. While training the former, a recognition netwrk, q_ϕ , learns a low-dimensional latent representation (\mathbf{z}) by modeling the ground truth set of future displacements ($\mathbf{d}\mathbf{y}$). During inference, it works like the conditional generator in cGAN therefore, we sample this latent vector from a standard Gaussian Distribution. Afterward, we concatenate the latent representation to the temporal hidden representation learned by the feature extractor (f_e). Finally, we autoregressively generate future displacements by decoding the last displacement vector and using f_e .

To optimize the cVAE, we use a weighted sum of a reconstruction loss, given by the MSE loss, and a regularization loss (Kullback-Liebler divergence) encouraging the learned distribution to match the prior distribution

$$L_V = \lambda \text{MSE}(\mathbf{y}, \hat{\mathbf{y}}) - (1 - \lambda) \beta D_{KL}[q_\phi(\mathbf{z}|\mathbf{d}\mathbf{y}, c) \| p(\mathbf{z}|\mathbf{d}\mathbf{x}, c)], \quad (4)$$

where β is the weight applied to the regularization loss, $q_\phi(\mathbf{z}|\mathbf{d}\mathbf{y}, c)$ and $p(\mathbf{z}|\mathbf{d}\mathbf{x}, c)$ are the recognition and predictor networks, respectively. For the recognition network, we employ an LSTM followed by linear layers. The predictor, on the other hand, utilizes an MLP to embed the input, an LSTM to extract temporal features, and an MLP to generate the predictions.

To achieve optimal performance of the cGAN, we adopt Eq. 3 for optimization. However, it should be noted that unlike the FP SC-GAN approach, the cGAN acts as a forecaster. Consequently, the inputs for the MSE and discriminator losses consist of future *tracklets*.

During inference, the trained cDGMS output a set of K possible displacement vectors, $\{\hat{\mathbf{d}}\mathbf{y}_i\}^K$. This set is the input of the last component in the system — ranking proposals — where we assign likelihoods to each item.

D. Ranking Proposals Step

The final step of the system aims to provide the mapping $\{\hat{\mathbf{d}}\mathbf{y}_i\}^K \rightarrow \{p_i\}^K$, which means assigning probabilities to the respective K predicted samples from each of the existing clusters. As mentioned before, the mapping to the probability space should ensure that samples from the right cluster have higher probabilities when compared to samples from the remaining clusters. To cope with this, one could train a deep neural network to learn the mapping $\{\hat{\mathbf{d}}\mathbf{y}_i\}^K \rightarrow \{p_i\}^K$ by itself [22], [23]. Alternatively, we propose mechanisms that rely on distance-based similarity measures: *centroids* and *neighbors*. For both methods, we consider the inverse relationship between the distance and the similarity between samples. For instance, the smaller the distance to a cluster's centroid, the greater the similarity to the samples of that cluster. Similarly, in *neighbors*, we hypothesize that the smaller the distance to N_{neig} neighbors from the same cluster, the greater the similarity to those samples and so a higher probability of belonging to that cluster. Formally, in distance-based methods, the probability of prediction $\hat{\mathbf{d}}\mathbf{y}_i$ belonging to the respective conditioning cluster, c_i , is given by:

$$\hat{p}_{c_i} = \frac{\exp(\frac{1}{m_{c_i}}/\tau)}{\sum_j^K \exp(\frac{1}{m_{c_j}}/\tau)}, \quad (5)$$

which is the soft-argmax function over the inverse of the distances, m . For the *centroids* approach, m_{c_i} corresponds to the L2-distance to the conditioning cluster's centroid, c_i . For the *neighbors* approach, m_{c_i} is the average L2-distance to the N_{neig} closest neighbors from cluster c_i . Formally, it is given as follows:

$$m_{c_i} = \frac{1}{N_{neig}} \sum_j^{N_{neig}} L2(\hat{\mathbf{d}}\mathbf{y}_i, \mathbf{d}\mathbf{y}_j) \quad (6)$$

We also evaluate a deep neural network [22], [23]. To this end, after training the cDGM, we use it to generate a dataset of displacements following the clustering space distribution. Then, we train a simple MLP that learns to classify the generated samples into the respective pseudo-labels given by the cluster assignments with the cross-entropy loss.

IV. EXPERIMENTS

In this section we compare our proposed methods and current baselines in different settings. Firstly, we describe the datasets, the baselines, and the assessment metrics. Secondly, we show and analyze quantitatively and qualitatively the results obtained in those datasets. Finally, we thoroughly analyze the ranking proposals methods.

A. Datasets, Baselines, and Metrics

We use two settings to evaluate our methods: train-test split and leave-one-dataset-out approach. For the former, we use two datasets: THÖR [37] and Argoverse [38]. THÖR is a human trajectory dataset, where the participants' roles — *visitors*, *workers*, and *inspector* — are scripted. We preprocess the raw data as in [26], so we end up with 2052 trajectories for training, 439 for validation, and 441 for testing. Moreover, following the current benchmarks [18], we create trajectories of 8-time steps of observation (3.2 s) and 12-time steps of forecasting (4.8 s). Argoverse is a road agents trajectory dataset, where there are also supervised classes: autonomous vehicles (*av*), regular vehicles (*agents*), and other road agents (*others*). For this dataset, analogously to [26], we sample 5726, 2100, and 1678 trajectories for training, validation, and testing sets, respectively. Additionally, we perform the leave-one-dataset-out in the widely used ETH/UCY benchmark [39], [40]. In this benchmark, similarly to THÖR, the observation length is 8-time steps (3.2 s) and the prediction length is 12-time steps (4.8 s). This benchmark comprises five datasets — ETH, HOTEL, UNIV, ZARA1, and ZARA2 — of which four are used to train the model and the remaining is left for testing. We use no overlapping between segments of entire trajectories.

We conduct the experiments with baselines widely used in scientific works in the trajectory prediction field:

- Constant Velocity Model (*CVM*) [20] — heuristic model that assumes that the humans move with constant velocity and direction. In this work we also include its comparison in road agents' data (Argoverse). In [20], the velocity is given by the projection of the last displacement but we use a weighted sum of the previous displacements based on a Gaussian kernel provided by [41]. Both methods achieve similar results.
- RED-LSTM predictor (*RED*) [19] — it is a stack of an LSTM (64 hidden dimensions) and a 2-layer MLP (hidden dimensions in $\{32, 16\}$) that receives linearly embedded displacements (linear layer with 16 hidden dimensions). After every layer, we use a PreLU activation function.
- Context-free GAN (*CF-GAN*) and Context-free VAE (*CF-VAE*) [18] — deep generative approaches based

on [18] but we remove any mechanisms that aim to model social interactions since we are solely interested in seeing the potential of trajectory-related additional information. *CF-VAE*, *CF-GAN*, and our deep generative proposals methods described in Sec. III-C have the same design choice: initial linear layer with 16 hidden dimensions, an LSTM with 64 hidden dimensions and a final linear layer with 32 hidden dimensions to decode the temporal features. To investigate the ability to generate a wide range of plausible trajectories, we incorporate the *k*-variety loss introduced in [17], as a replacement for the MSE partial loss utilized in the generator's loss (in the case of *CF-GAN*) and the VAE's loss (in the case of *CF-VAE*).

As described in Section III-C, we compare two cDGMs: cVAE (*OURS-VAE*) and cGAN (*OURS-GAN*). Additionally, we evaluate three clustering algorithms: *k-Means*, *TS k-Means*, and the proposed *FP SC-GAN*. Furthermore, we have three ranking proposals methods: (1) based on the Euclidean distance to the centroids (*cent*); (2) based on the Euclidean distance to the N_{neig} closest neighbors (set to 20) in the displacement space and feature space, denoted as *neigh-ds* and *neigh-fs*, respectively. It is important to note here that *neigh-fs* is only used in *FP SC-GAN* as it is the unique method that makes use of a deep feature space; (3) based on the classification provided by the auxiliary network (*anet*). As our methods rely on a clustering process, we need to determine the number of clusters in each dataset. To do so, we average the results of five runs of each clustering method. For the remaining experiments, we use the number of clusters that yields the smallest Davies–Bouldin Index (DBI) [42].

The metrics we use to compare the different methods rely on Average Displacement Error (ADE) that measures the average Euclidean distance between the predicted positions and the ground truth and the Final Displacement Error (FDE) that measures the Euclidean distance between the final predicted position and the respective ground truth (at $t = T_P$). To compare both deterministic point estimate predictors (*CVM* and *RED*) to stochastic multimodal models (*CF-GAN*, *CF-VAE*, *VAE-OURS*, and *GAN-OURS*), we provide the following metrics:

- 1) Top-3 ADE/FDE (in meters) — used to assess the multimodal estimates produced by generative models. From *CF-GAN* and *CF-VAE*, we sample 3 trajectories and evaluate the closest one to the ground truth, whereas from *GAN-OURS* and *VAE-OURS*, we take the 3 most likely trajectories and compare the closest one to the ground truth.
- 2) Top-1 ADE/FDE (in meters) — used to compare point estimate predictors to stochastic multimodal models. From *CF-GAN* and *CF-VAE*, we use the first prediction generated by the models, while from *GAN-OURS* and *VAE-OURS*, we use the most likely trajectory.

Finally, to compare the ranking proposals methods, we use accuracy (in %). In this case we compare the output of the ranking proposals methods to the soft labels yielded by each

TABLE I

TOP-3 ADE/FDE (\downarrow) METRICS IN THE TEST SETS.

Datasets	<i>CF-GAN</i>	<i>GAN-OURS</i> ¹	<i>CF-VAE</i>	<i>VAE-OURS</i> ¹
THÖR	0.57 ± 0.01	0.53 ± 0.01	0.62 ± 0.02	0.56 ± 0.01
	1.04 ± 0.03	0.84 ± 0.03	1.05 ± 0.05	0.89 ± 0.02
Argoverse	1.62 ± 0.07	1.56 ± 0.02	1.96 ± 0.02	1.62 ± 0.02
	2.81 ± 0.14	2.69 ± 0.02	3.44 ± 0.06	2.82 ± 0.04
ETH	0.84 ± 0.03	0.77 ± 0.04	0.94 ± 0.02	0.82 ± 0.02
	1.64 ± 0.06	1.60 ± 0.11	1.84 ± 0.04	1.60 ± 0.04
HOTEL	0.87 ± 0.07	0.81 ± 0.10	1.08 ± 0.04	0.97 ± 0.08
	1.64 ± 0.12	1.46 ± 0.11	1.95 ± 0.06	1.72 ± 0.14
UNIV	0.56 ± 0.01	0.51 ± 0.01	0.61 ± 0.01	0.56 ± 0.01
	1.08 ± 0.02	0.98 ± 0.03	1.16 ± 0.01	1.06 ± 0.02
ZARA1	0.43 ± 0.02	0.37 ± 0.01	0.48 ± 0.01	0.44 ± 0.01
	0.82 ± 0.07	0.72 ± 0.03	0.98 ± 0.04	0.91 ± 0.03
ZARA2	0.46 ± 0.01	0.40 ± 0.01	0.49 ± 0.01	0.43 ± 0.01
	0.81 ± 0.05	0.65 ± 0.03	0.86 ± 0.05	0.73 ± 0.01

¹*FP SC-GAN + neig-fs*

clustering method.

B. Results

In this section we show the results obtained by our methods and the baselines in the datasets, where bold scores denote the best score, and the results from Deep Learning (DL)-based approaches are averaged over five runs. First, as the main focus of our approach is to generate a probabilistic yet accurate set of predictions, we depict in Tab. I the Top-3 ADE/FDE results for deep generative approaches. Our methodology exhibits superior performance compared to the baseline models across all datasets, indicating that among the three most probable predicted trajectories, our system produces a more accurate prediction. This finding reinforces the notion that generating multimodality within the conditioning cluster, as opposed to relying on the latent space learned through the *k*-variety loss, leads to improved outcomes. Furthermore, it is noteworthy to mention that the various clustering methods and ranking proposal mechanisms yield similar results across the datasets. However, in some specific datasets, one can find better results in other configurations: in THÖR with *GAN-OURS*, *cent* yields 0.45 ± 0.02 and 0.75 ± 0.03 and in ZARA2 where *TS k-Means* followed by *neig* yields 0.37 ± 0.01 and 0.62 ± 0.01 , for ADE and FDE, respectively.

The fact that our system performs better on the leave-one-dataset-out setting suggests that the clusters are unbiased to the reference dataset. In particular, Tab. II shows the results in the HOTEL dataset with *GAN-OURS*, where the trajectories go in a different direction than most of the ones in the training set [20]. Here we can see that the proposed *FP SC-GAN* is more robust to the distribution shift present in this dataset.

To assess the variability of each model and the fine-grained accuracy, we also provide in Tab. III the Top-1 ADE/FDE scores. Apart from HOTEL, this result shows that our method yields similar Top-1 predictions to point estimate and multimodal baselines, where *RED* stood out

TABLE II

TOP-3 ADE/FDE (\downarrow) METRICS IN HOTEL WITH *GAN-OURS*.

Ranking proposals	<i>K-means</i>	<i>TS K-means</i>	<i>FP SC-GAN</i>
<i>cent</i>	1.03 ± 0.05	1.04 ± 0.05	0.80 ± 0.10
	1.80 ± 0.09	1.81 ± 0.06	1.44 ± 0.12
<i>neig</i> ¹	0.98 ± 0.04	0.97 ± 0.11	0.81 ± 0.10
	1.74 ± 0.06	1.71 ± 0.16	1.46 ± 0.11
<i>anet</i>	1.02 ± 0.06	0.97 ± 0.04	0.90 ± 0.06
	1.78 ± 0.10	1.70 ± 0.04	1.59 ± 0.08

¹*neigh-ds* for *k-Means* and *TS K-means*; *neigh-fs* for *FP SC-GAN*TABLE III
TOP-1 ADE/FDE (\downarrow) METRICS IN THE TEST SETS.

Datasets	<i>CVM</i>	<i>RED</i>	<i>CF-GAN</i>	<i>GAN-OURS</i> ¹	<i>VAE</i>	<i>VAE-OURS</i> ¹
THÖR	0.79	0.65 ± 0.01	0.85 ± 0.09	0.76 ± 0.02	0.71 ± 0.02	0.71 ± 0.02
	1.28	1.06 ± 0.01	1.68 ± 0.20	1.31 ± 0.05	1.30 ± 0.04	1.21 ± 0.04
Argoverse	2.57	1.84 ± 0.01	2.41 ± 0.09	1.92 ± 0.02	2.69 ± 0.02	1.95 ± 0.01
	3.93	3.18 ± 0.02	4.53 ± 0.17	3.27 ± 0.03	4.94 ± 0.02	3.39 ± 0.04
ETH	0.95	0.95 ± 0.01	1.08 ± 0.08	0.96 ± 0.03	1.08 ± 0.03	0.95 ± 0.02
	2.11	1.94 ± 0.02	2.18 ± 0.19	1.99 ± 0.05	2.15 ± 0.08	1.95 ± 0.03
HOTEL	0.42	1.03 ± 0.04	1.03 ± 0.05	0.95 ± 0.13	1.18 ± 0.05	1.09 ± 0.12
	0.74	1.84 ± 0.06	1.99 ± 0.11	1.72 ± 0.19	2.21 ± 0.08	1.96 ± 0.18
UNIV	0.65	0.65 ± 0.01	0.74 ± 0.03	0.74 ± 0.01	0.71 ± 0.01	0.69 ± 0.01
	1.29	1.27 ± 0.01	1.49 ± 0.05	1.44 ± 0.04	1.41 ± 0.01	1.36 ± 0.01
ZARA1	0.54	0.45 ± 0.01	0.60 ± 0.11	0.47 ± 0.01	0.64 ± 0.01	0.53 ± 0.01
	1.05	0.87 ± 0.01	1.21 ± 0.24	0.92 ± 0.03	1.33 ± 0.03	1.10 ± 0.02
ZARA2	0.55	0.50 ± 0.01	0.65 ± 0.02	0.52 ± 0.01	0.60 ± 0.02	0.54 ± 0.01
	0.91	0.80 ± 0.01	1.24 ± 0.09	0.86 ± 0.04	1.13 ± 0.07	0.93 ± 0.01

¹*FP SC-GAN + neig-fs*

the most. Nevertheless, when considering a comparison between the generative models *CF-GAN* and *CF-VAE* and our proposed methods *GAN-OURS* and *VAE-OURS*, which share the same network structure, our methods demonstrate superior performance in terms of Top-3 scores across all datasets. Additionally, our methods achieve equal or superior Top-1 scores in all datasets. Notably, our methods also effectively alleviate the performance disparity resulting from the models' variability when comparing Top-3 and Top-1 results. On top of that, our methods yield more information encoded in the probabilities assigned to the predicted trajectories, thus, creating a space of probable future locations rather than uninformative predictions. It is also interesting to note that *CVM* provides similar or better performance in human trajectory data. However, for road agents' trajectory data, this method cannot cope with the speed variation in the trajectories.

In Fig. 3, we show qualitative results of the Top-3 predictions from our methods and baselines in THÖR (left), Argoverse (center), and ZARA1 (right) test sets. THÖR example pertains to a quite challenging scenario as the heading change is sharp. Still, our method could capture this uncommon behavior within the three most probable trajectories (with $p = 0.26$), while the most probable trajectory ($p = 0.48$) is following the movement's trend, which is reasonable due to the most common constant velocity profile in humans walking [20]. In Argoverse example, the auxiliary network plays an important role in the hierarchical predictions: Top-1 prediction ($p_1 = 0.29$) is also the closest to the ground truth; the second most likely trajectory ($p_4 = 0.23$) is following the

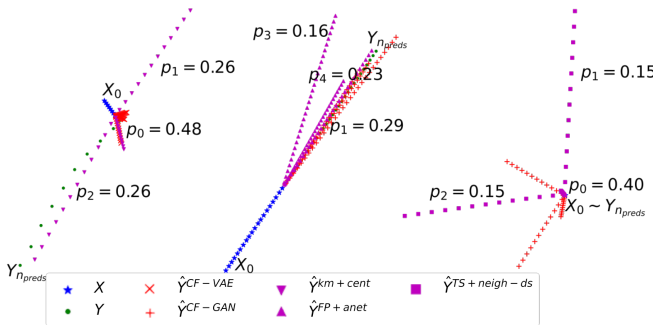


Fig. 3. Top-3 predictions in test samples from THÖR (left), Argoverse (center), and ZARA2 (right). X_0 denotes the first observed point, $Y_{n_{pred}}$ denotes the last point of the ground-truth, and $p_i \in [0, K-1]$ the probabilities provided by our ranking proposals methods.

same direction but with a shorter distance; finally, the third most likely trajectory ($p = 0.16$) goes in a different direction, but we consider it a still reasonable prediction. Finally, in ZARA2 example, while *CF-GAN* could not capture the static behavior ($X_0 \sim Y_{n_{pred}}$) but still yields a broad range of behaviors, our method conditioned by the cluster id assigns the highest likelihood to the predicted static behavior ($p = 0.40$).

C. Ranking Proposals Analysis

In this section, we analyze the ranking proposals methods with the estimates from *GAN-OURS*. Tab. IV shows the accuracy of the ranking proposals methods in the test sets of the train test split settings (THÖR and Argoverse). It is evident that the accuracy of the ranking proposals methods directly affects both Top-3 and Top-1 results presented in Tab. I and Tab. III, respectively. A broad view of the results shows that the more accurate our ranking proposals methods are, the better the ADE/FDE scores, specially Top-1 ADE/FDE. As it is possible to observe within each clustering method and dataset, *anet* is (statistically) better only in THÖR for all clustering methods. We speculate that this may be because the clusters in THÖR are closer to each other as people were moving in the same environment (with similar moving patterns) in both train and test sets. This phenomenon is less noticeable in Argoverse since different behaviors stem from cars (*agents* and *av*) and other road agents (*others*). Similarly, in the leave-one-dataset-out setting (see Tab. V), the diversity of behaviors come from the different datasets. In the majority of these datasets, our proposed distance-based methods (*cent*, *neigh-ds* and *neigh-fs*) provide better results than an auxiliary deep neural network (*anet*) across the different clustering methods. Furthermore, while a constant-width MLP-based *anet* provides accurate estimates, it computationally scales as $\mathcal{O}(N_L H_U^2)$, where N_L is the number of layers of the MLP network and H_U is the number of hidden units per layer. On the contrary, distance-based methods, *centroids* and *neighbors*, require $\mathcal{O}(K)$ and $\mathcal{O}(K N_{neig})$ computations, respectively. Hence, besides the fact that distance-based methods do not require training an additional neural network, during inference, they provide similar performance in *linear*

TABLE IV
ACCURACY (\uparrow) OF THE RANKING PROPOSALS METHODS IN THE TEST SETS OF THE TRAN TEST SPLIT SETTING.

Clustering method	Ranking proposals	THÖR	Argoverse
		cent	93.0 \pm 0.5
<i>k</i> -Means	neigh-ds	81.1 \pm 0.8	94.0 \pm 0.2
	anet	86.6 \pm 0.6	95.2 \pm 0.2
	cent	66.4 \pm 0.4	93.9 \pm 0.9
TS <i>k</i> -Means	neigh-ds	65.8 \pm 0.4	94.6 \pm 0.3
	anet	72.7 \pm 0.8	96.0 \pm 0.1
	cent	64.3 \pm 5.6	96.5 \pm 0.4
FP SC-GAN	neigh-fs	68.0 \pm 2.7	96.3 \pm 5.1
	anet	70.3 \pm 1.3	94.9 \pm 0.7

TABLE V
ACCURACY (\uparrow) OF THE RANKING PROPOSALS METHODS IN THE TEST SETS IN THE LEAVE-ONE-DATASET-OUT SETTING.

Clustering method	Ranking proposals	ETH	HOTEL	UNIV	ZARA1	ZARA2
<i>k</i> -Means	cent	94.9 \pm 1.0	100.0 \pm 0.0	84.0 \pm 0.4	92.8 \pm 0.2	94.7 \pm 0.3
	neigh-ds	97.7 \pm 0.8	99.2 \pm 0.3	80.8 \pm 1.0	89.7 \pm 0.9	95.5 \pm 0.2
	anet	93.3 \pm 2.0	98.6 \pm 0.4	82.5 \pm 0.9	93.9 \pm 0.9	95.2 \pm 0.4
TS <i>k</i> -Means	cent	95.3 \pm 1.0	100.0 \pm 0.0	86.6 \pm 0.2	92.5 \pm 0.2	94.5 \pm 0.1
	neigh-ds	97.7 \pm 0.8	99.3 \pm 0.0	82.0 \pm 0.9	90.6 \pm 0.6	94.9 \pm 0.1
	anet	94.5 \pm 0.8	98.3 \pm 0.6	84.1 \pm 0.4	93.2 \pm 0.6	95.0 \pm 0.3
FP SC-GAN	cent	70.2 \pm 11.2	78.8 \pm 8.7	64.9 \pm 2.1	90.6 \pm 3.5	91.4 \pm 4.0
	neigh-fs	75.3 \pm 5.3	90.6 \pm 6.2	65.2 \pm 2.8	89.7 \pm 5.1	89.2 \pm 2.2
	anet	68.6 \pm 8.0	83.3 \pm 7.9	55.8 \pm 2.6	90.6 \pm 2.7	90.2 \pm 3.2

time while auxiliary networks require *quadratic* time.

V. CONCLUSION

In this paper, we propose a multi-stage probabilistic trajectory predictor: displacement space transformation, clustering stage, proposals generation, and ranking proposals. At the clustering stage, we propose a novel trajectory clustering method (FP SC-GAN) based on deep features from a GAN framework. We also propose distance-based ranking proposals methods for assigning probabilities to the predictions.

We test our methods in two settings: train-test split and leave-one-dataset-out. The former comprise human and road agents' trajectory data, while the latter only address pedestrians' trajectory data. Experimental results show that our system surpasses the multimodal generative baselines (with *k*-variety loss) in Top-3 ADE/FDE scores. It also performs equally or better than context-free generative baselines in Top-1 ADE/FDE scores. Moreover, the proposed clustering method copes better with distributional shifts (HOTEL dataset) than traditional clustering methods. Finally, our ranking proposals methods based on distance similarity measures perform globally better than auxiliary deep neural networks. It is even more remarkable since these mechanisms do not require training an additional neural network and run in *linear* time, while a constant-width MLP runs in *quadratic* time.

REFERENCES

- [1] J. J. Q. Yu, "Graph construction for traffic prediction: A data-driven approach," *IEEE Trans. on Intell. Transp. Syst.*, vol. 23, no. 9, pp. 15 015–15 027, 2022.
- [2] F. Li, J. Feng, H. Yan, G. Jin, F. Yang, F. Sun, D. Jin, and Y. Li, "Dynamic graph convolutional recurrent network for traffic prediction: Benchmark and solution," *ACM Trans. Knowl. Discov. Data*, vol. 17, no. 1, feb 2023.

[3] D. Singh and R. Srivastava, "Graph neural network with rnns based trajectory prediction of dynamic agents for autonomous vehicle," *Appl. Intell.*, vol. 52, no. 11, p. 12801–12816, sep 2022.

[4] A. Dalgkitis, P.-V. Mekikis, A. Antonopoulos, and C. Verikoukis, "Data driven service orchestration for vehicular networks," *IEEE Trans. on Intell. Transp. Syst.*, vol. 22, no. 7, pp. 4100–4109, 2021.

[5] J. Dahl, G. R. d. Campos, and J. Fredriksson, "Prediction-uncertainty-aware threat detection foradas: A case study on lane-keeping assistance," *IEEE Trans. on Intell. Vehicles*, pp. 1–12, 2023.

[6] V. Kosaraju, A. Sadeghian, R. Martín-Martín, I. Reid, S. H. Rezatofighi, and S. Savarese, *Social-BiGAT: Multimodal Trajectory Forecasting Using Bicycle-GAN and Graph Attention Networks*. Red Hook, NY, USA: Curran Associates Inc., 2019.

[7] A. Sadeghian, V. Kosaraju, A. Sadeghian, N. Hirose, H. Rezatofighi, and S. Savarese, "Sophie: An attentive gan for predicting paths compliant to social and physical constraints," in *2019 IEEE/CVF Conf. on Comput. Vision and Pattern Recognit. (CVPR)*, 2019, pp. 1349–1358.

[8] H. Tang, P. Wei, J. Li, and N. Zheng, "Evostgat: Evolving spatiotemporal graph attention networks for pedestrian trajectory prediction," *Neurocomputing*, vol. 491, pp. 333–342, 2022.

[9] Y. Su, J. Du, Y. Li, X. Li, R. Liang, Z. Hua, and J. Zhou, "Trajectory forecasting based on prior-aware directed graph convolutional neural network," *IEEE Trans. on Intell. Transp. Syst.*, vol. 23, no. 9, pp. 16 773–16 785, 2022.

[10] H. Minoura, T. Hirakawa, Y. Sugano, T. Yamashita, and H. Fujiyoshi, "Utilizing human social norms for multimodal trajectory forecasting via group-based forecasting module," *IEEE Trans. on Intell. Vehicles*, vol. 8, no. 1, pp. 836–850, 2023.

[11] P. Kothari and A. Alahi, "Safety-compliant generative adversarial networks for human trajectory forecasting," *IEEE Trans. on Intell. Transp. Syst.*, vol. 24, no. 4, pp. 4251–4261, 2023.

[12] B. Xia, C. Wong, Q. Peng, W. Yuan, and X. You, "Cscnet: Contextual semantic consistency network for trajectory prediction in crowded spaces," *Pattern Recognit.*, vol. 126, p. 108552, 2022.

[13] V. Kress, F. Jeske, S. Zernetsch, K. Doll, and B. Sick, "Pose and semantic map based probabilistic forecast of vulnerable road users' trajectories," *IEEE Trans. on Intell. Vehicles*, vol. 8, no. 3, pp. 2592–2603, 2023.

[14] N. Deo, E. Wolff, and O. Beijbom, "Multimodal trajectory prediction conditioned on lane-graph traversals," in *Proceedings of the 5th Conf. on Robot Learning*, ser. Proceedings of Mach. Learning Research, A. Faust, D. Hsu, and G. Neumann, Eds., vol. 164. PMLR, 08–11 Nov 2022, pp. 203–212.

[15] I. Bae, J.-H. Park, and H.-G. Jeon, "Non-probability sampling network for stochastic human trajectory prediction," in *Proceedings of the IEEE/CVF Conf. on Comput. Vision and Pattern Recognit. (CVPR)*, June 2022, pp. 6477–6487.

[16] W. Chen, F. Zheng, L. Shi, Y. Zhi, H. Sun, and N. Zheng, "Multiple goals network for pedestrian trajectory prediction in autonomous driving," in *2022 IEEE 25th Int. Conf. on Intell. Transp. Syst. (ITSC)*. IEEE Press, 2022, p. 717–722.

[17] A. Gupta, J. Johnson, L. Fei-Fei, S. Savarese, and A. Alahi, "Social gan: Socially acceptable trajectories with generative adversarial networks," in *IEEE/CVF Conf. on Comput. Vision and Pattern Recognit.*, 2018, pp. 2255–2264.

[18] P. Kothari, S. Kreiss, and A. Alahi, "Human trajectory forecasting in crowds: A deep learning perspective," *IEEE Trans. on Intell. Transp. Syst.*, pp. 1–15, 2020.

[19] S. Becker, R. Hug, W. Hübner, and M. Arens, "Red: A simple but effective baseline predictor for the trajnet benchmark," in *ECCV Workshops*, 2018.

[20] C. Schöller, V. Aravantinos, F. Lay, and A. Knoll, "What the constant velocity model can teach us about pedestrian motion prediction," *IEEE Robot. and Automat. Lett.*, vol. 5, no. 2, pp. 1696–1703, 2020.

[21] F. Giuliani, I. Hasan, M. Cristani, and F. Galasso, "Transformer networks for trajectory forecasting," in *2020 25th Int. Conf. on Pattern Recognit. (ICPR)*. Los Alamitos, CA, USA: IEEE Comput. Society, jan 2021, pp. 10 335–10 342.

[22] J. Sun, Y. Li, H. Fang, and C. Lu, "Three steps to multimodal trajectory prediction: Modality clustering, classification and synthesis," *2021 IEEE/CVF Int. Conf. on Comput. Vision (ICCV)*, pp. 13 230–13 239, 2021.

[23] W. Chen, Z. Yang, L. Xue, J. Duan, H. Sun, and N. Zheng, "Multimodal pedestrian trajectory prediction using probabilistic proposal network," *IEEE Trans. on Circuits and Syst. for Video Technology*, pp. 1–1, 2022.

[24] M. Kang, J. Fu, S. Zhou, S. Zhang, and N. Zheng, "Learning to predict diverse trajectory from human motion patterns," *Neurocomputing*, vol. 504, pp. 123–131, 2022.

[25] S. Liu, T. Wang, D. Bau, J.-Y. Zhu, and A. Torralba, "Diverse image generation via self-conditioned gans," in *2020 IEEE/CVF Conf. on Comput. Vision and Pattern Recognit. (CVPR)*, 2020, pp. 14 274–14 283.

[26] T. Rodrigues de Almeida, E. Gutierrez Maestro, and O. Martinez Mazzos, "Context-free self-conditioned gan for trajectory forecasting," in *2022 21st IEEE Int. Conf. on Mach. Learning and Applications (ICMLA)*, 2022, pp. 1218–1223.

[27] P. Dendorfer, A. Osep, and L. Leal-Taixé, "Goal-gan: Multimodal trajectory prediction based on goal position estimation," in *Asian Conf. on Comput. Vision (ACCV)*, 2021, pp. 405–420.

[28] H. Sun, Z. Zhao, and Z. He, "Reciprocal learning networks for human trajectory prediction," in *2020 IEEE/CVF Conf. on Comput. Vision and Pattern Recognit. (CVPR)*. Los Alamitos, CA, USA: IEEE Comput. Society, jun 2020, pp. 7414–7423.

[29] T. Salzmann, B. Ivanovic, P. Chakravarty, and M. Pavone, "Trajettron++: Dynamically-Feasible Trajectory Forecasting With Heterogeneous Data," *arXiv e-prints*, p. arXiv:2001.03093, Jan. 2020.

[30] T. Phan-Minh, E. C. Grigore, F. A. Boulton, O. Beijbom, and E. M. Wolff, "Covernet: Multimodal behavior prediction using trajectory sets," in *2020 IEEE/CVF Conf. on Comput. Vision and Pattern Recognit. (CVPR)*, 2020, pp. 14 062–14 071.

[31] Y. Ma, J. Inala, D. Jayaraman, and O. Bastani, "Likelihood-based diverse sampling for trajectory forecasting," in *2021 IEEE/CVF Int. Conf. on Comput. Vision (ICCV)*. Los Alamitos, CA, USA: IEEE Comput. Society, oct 2021, pp. 13 259–13 268.

[32] B. Ivanovic, K.-H. Lee, P. Tokmakov, B. Wulfe, R. McAllister, A. Gaidon, and M. Pavone, "Heterogeneous-agent trajectory forecasting incorporating class uncertainty," in *2022 IEEE/RSJ Int. Conf. on Intell. Robots and Syst. (IROS)*, 2022, pp. 12 196–12 203.

[33] L. Calem, H. Ben-Younes, P. Pérez, and N. Thome, "Diverse probabilistic trajectory forecasting with admissibility constraints," in *2022 26th Int. Conf. on Pattern Recognit. (ICPR)*, 2022, pp. 3478–3484.

[34] X. Jin and J. Han, *K-Means Clustering*. Springer US, 2010, pp. 563–564.

[35] R. Tavenard, J. Faouzi, G. Vandewiele, F. Divo, G. Androz, C. Holtz, M. Payne, R. Yurchak, M. Rußwurm, K. Kolar, and E. Woods, "Tslearn, a mach. learning toolkit for time series data," *Journal of Mach. Learning Research*, vol. 21, no. 118, pp. 1–6, 2020.

[36] M. Cuturi and M. Blondel, "Soft-dtw: A differentiable loss function for time-series," in *Proceedings of the 34th Int. Conf. on Mach. Learning - Volume 70*, ser. ICML'17. JMLR.org, 2017, p. 894–903.

[37] A. Rudenko, T. P. Kucner, C. S. Swaminathan, R. T. Chadalavada, K. O. Arras, and A. J. Lilienthal, "Thör: Human-robot navigation data collection and accurate motion trajectories dataset," *IEEE Robot. and Automat. Lett.*, vol. 5, no. 2, pp. 676–682, 2020.

[38] M.-F. Chang, J. W. Lambert, P. Sangkloy, J. Singh, S. Bak, A. Hartnett, D. Wang, P. Carr, S. Lucey, D. Ramanan, and J. Hays, "Argoverse: 3d tracking and forecasting with rich maps," in *IEEE/CVF Conf. on Comput. Vision and Pattern Recognit.*, 2019.

[39] S. Pellegrini, A. Ess, K. Schindler, and L. van Gool, "You'll never walk alone: Modeling social behavior for multi-target tracking," in *2009 IEEE 12th Int. Conf. on Comput. Vision*, 2009, pp. 261–268.

[40] L. Leal-Taixé, M. Fenzi, A. Kuznetsova, B. Rosenhahn, and S. Savarese, "Learning an image-based motion context for multiple people tracking," in *2014 IEEE Conf. on Comput. Vision and Pattern Recognit.*, 2014, pp. 3542–3549.

[41] A. Rudenko, W. Huang, L. Palmieri, K. O. Arras, and A. Lilienthal, "Atlas: a benchmarking tool for human motion prediction algorithms," in *Robot.: Sci. and Syst.*, 2021.

[42] D. L. Davies and D. W. Bouldin, "A cluster separation measure," *IEEE Trans. on Pattern Anal. and Mach. Intell.*, vol. PAMI-1, no. 2, pp. 224–227, 1979.